Journal of Geoscience and Environment Protection, 2025, 13(1), 260-291
https://www.scirp.org/journal/gep
ISSN Online: 2327-4344
ISSN Print: 2327-4336

Interannual Variability of the NDVI in East Africa during 1983-2022 and the Climate Impact

Emmanuel Lusoloja Mabula[1,2], Yi Fan[1*], Daniel Stephene Semgomba[1,3]

[1]Key Laboratory of Meteorology Disaster, Ministry of Education (KLME), Joint International Research Laboratory of Climate and Environment Change (ILCEC), Collaborative Innovation Center on Forecast and Evaluation of Meteorological Disasters (CIC-FEMD), Nanjing University of Information Science and Technology, Nanjing, China
[2]Tanzania Meteorological Authority (TMA), Kilimanjaro International Airport (KIA), Kilimanjaro, Tanzania
[3]Tanzania Meteorological Authority (TMA), Dar-es-Salaam, Tanzania
Email: emmanuelmabula10@gmail.com, *fanyi@nuist.edu.cn

How to cite this paper: Mabula, E. L., Fan, Y., & Semgomba, D. S. (2025). Interannual Variability of the NDVI in East Africa during 1983-2022 and the Climate Impact. *Journal of Geoscience and Environment Protection, 13,* 260-291.
https://doi.org/10.4236/gep.2025.131014

Received: December 5, 2024
Accepted: January 20, 2025
Published: January 23, 2025

Abstract

The interannual variability of Normalized Difference Vegetation Index (NDVI) over East Africa demonstrates the complex interactions between vegetation dynamics and climatic factors. This study, which spans the period from 1983 to 2022, makes use of data from NOAA, ERA5, and CRU. It employs a range of statistical techniques, including the calculation of standardized anomalies, significance testing, composites and correlation analyses. The results demonstrated an increase in NDVI over regions including Kenya, Central and Northeastern Tanzania during wet years, with significantly higher NDVI compared to drought years. Conversely, regions such as Uganda, Rwanda, Burundi, and parts of western and southern Tanzania exhibited lower NDVI during wet years than in drought years, thereby underscoring the existence of significant regional differences in vegetation responses to climatic conditions. The results of the correlation analysis indicated that there was a negative correlation between NDVI and SLHF, air temperature, and soil temperature, while positive correlations were observed between NDVI and SSHF, precipitation, and soil moisture. Furthermore, teleconnections with large-scale climate indices demonstrated modest correlations: Niño 3.4 (r = 0.33), DMI (r = 0.11), and AMO (r = 0.03). These findings emphasize the pivotal role of climatic and meteorological factors in influencing vegetation dynamics, offering insights for sustainable land management and climate adaptation strategies in East Africa.

Keywords

East Africa, NDVI, Interannual Variability, Wet Years, Drought Years

1. Introduction

The interannual variation of the Normalized Difference Vegetation Index (NDVI) is strongly influenced by a variety of climatic factors, including precipitation and temperature, highlighting the existence of complex interactions across different time scales. NDVI derived from satellite imagery is a key metric for assessing the state of live green vegetation growth and understanding the response of vegetation dynamics to climatic variations (Walther et al., 2002), the application of this technique is particularly beneficial for the monitoring of vegetative dynamics, productivity patterns and spatial distribution, which are fundamental elements in the field of ecological research. Furthermore, it is a commonly employed metric that is based on the proportional relationship between red (R) and near-infrared (NIR) reflectance, which is expressed mathematically as follows: NDVI = (NIR − R)/(NIR + R) (Tucker et al., 2005). This quantitative indicator evaluates both vegetated and non-vegetated landforms on a spectrum ranging from +1 to −1, with elevated NDVI values (approaching +1) indicating the presence of dense, thriving green vegetation, and lower values indicating vegetation under moisture stress (Gessesse & Melesse, 2019).

Fluctuations in the NDVI show a direct correlation with climatic changes, particularly those associated with precipitation and temperature variations (Ghebrezgabher et al., 2020; Yang et al., 2014). Precipitation emerges as a fundamental determinant of NDVI variability, in different regions, where precipitation history strongly influences vegetation productivity (Han et al., 2022; Mao et al., 2022). Temperature also has an influence on NDVI, typically showing a negative correlation, especially in arid landscapes where high temperatures can limit vegetation growth (Sonia et al., 2023; Zhang et al., 2023).

In addition, growing season sunshine duration plays an important role in modulating NDVI in different regions, where it interacts with precipitation to shape vegetation dynamics (Mao et al., 2022). The sensitivity of the NDVI to precipitation demonstrates variability depending on the specific type of vegetation, with shrubland and prairie ecosystems showing a pronounced response to fluctuations in precipitation, whereas forest and woodland vegetation show a comparatively muted response to changes in precipitation (Ding et al., 2007).

Nevertheless, large scale climate systems significantly influence the dynamics of vegetation change in response to global climate variability. The El Niño-Southern Oscillation (ENSO) is one of the most notable climate systems with significant impacts on global climatic conditions, ecological systems and social structures (Cane, 1983; Philander, 1983; Rasmusson & Wallace, 1983). It is a phenomenon linked to the ocean and atmosphere in the tropical Pacific and has been identified as the most important factor influencing global weather patterns. A fundamental aspect of Earth system science research is to understand the complex interactions between climate conditions and vegetation dynamics.

Vegetation occupies approximately 70% of the Earth's land surface and plays an essential role in regulating the balance of net radiation at the terrestrial inter-

face. NDVI affects the way in which this radiation is partitioned into sensible heat, latent heat and heat flux, and thus has a major influence on land atmosphere (Gray et al., 2018; Su et al., 2021; van Heerwaarden & Teuling, 2014; Zhang et al., 2019). In regard to radiative phenomena, the presence of vegetation can result in an increase in the roughness of the land surface, which may subsequently lead to a reduction in albedo (Pang et al., 2022), resulting in an increase in net radiation. In regard to non-radiative mechanisms, the presence of vegetation can increase evapotranspiration, leading to an increase in latent heat and a decrease in sensible heat (Duveiller et al., 2018). The interaction between land and atmosphere, as well as climatic conditions, is significantly influenced by both radiative and non-radiative changes associated with vegetation phenomena (Bonan, 2008).

Numerous scholars have investigated Interannual variability of NDVI and its relationship to climate factors (Paruelo & Lauenroth, 1998). The findings underscore the substantial influence of climatic variables on vegetation activity, with temperature and precipitation being key factors in different geographical regions. This study was further conducted in East Africa to examine the consequences of climate change on vegetation dynamics, as expressed by Kalisa et al. (2019), who propose that precipitation is a more dominant influence on vegetation development in East Africa than temperature.

Understanding NDVI is essential for assessing vegetation health. The benefits of this approach are widespread and extend to farmers, environmentalists and policy makers alike. They include improvements in agricultural practices, support for nature conservation and assistance with disaster management. Policy makers use the data to monitor productivity, allocate resources and assess the impact of climate change on sustainable management practices.

This research examines interannual variations in NDVI across East Africa from 1983 to 2022, a period characterised by significant climatic phenomena such as El Niño, La Niña and frequent droughts. Through a comprehensive annual assessment, this investigation aims to identify changes in vegetation cover and productivity, providing valuable insights into the stability of regional ecosystems. The results of this research will contribute to a deeper understanding of NDVI variability in relation to climatic influences, thereby facilitating sustainable land management and conservation initiatives in East Africa. This research is organized as follows: data and methodology are briefly explained in Section 2, Section 3 presents results and discussion on the Interannual Variability of NDVI in East Africa and Climate Impact. The conclusion is given in Section 4.

2. Data and Methodology

2.1. Study Area

The geographical domain of this research encompasses five countries: Tanzania, Kenya, Uganda, Rwanda, and Burundi. These countries are collectively referred to as East Africa (EA) and are situated between 5˚20'N and 11˚45'S, as well as between 28˚51'E and 41˚54'E (**Figure 1**). The region of EA encompasses an ex-

tensive area of 1.82 million square kilometers, eastern boundary with the Indian Ocean plays a pivotal role in the region's atmospheric moisture dynamics, acting as a crucial source of moisture for the region (Sheriff, 2017). The western region of East Africa is bounded by the Congo Basin, whose influence is considerable due to the formation of the Congo air-mass a warm, moist air-mass that is essential to the climatic dynamics of the region. As this moist tropical air mass moves eastwards, it transports significant amounts of atmospheric moisture into the regions of the EA. This influx of moisture greatly enhances convective activity, resulting in increased precipitation, especially during the wet season (Ward et al., 2023).

The EA region is distinguished by a diverse topography, encompassing elevations that vary by approximately 6,000 meters. The region is distinguished by a number of distinctive physical features, including the Rift Valley, Lake Victoria, Mount Kilimanjaro, and Mount Kenya (Ayugi et al., 2021). EA is predominantly semi-arid with an average rainfall amount of less than 800 mm per year; and sub-humid with an average rainfall amount varying between 800 and 1300 mm per year (Nicholson et al., 1990). The Inter-Tropical Convergence Zone (ITCZ) exerts a profound influence on the seasonal patterns of EA, which is characterized by two principal rainy seasons. The extended rainy period occurs from March to May (MAM), while the shorter rainy season spans from October to December (OND) (Ayugi et al., 2021; Kimani et al., 2017).

The region is distinguished by its elevated population density, which is among the highest in Africa. The economy is predominantly agricultural, with 80% of the population deriving their livelihoods from rainfed agriculture. As is the case in numerous other regions around the globe, it is of paramount importance to gain an understanding of the impact of climate change on the territories of EA, as evidenced by a substantial body of academic literature (Kalisa et al., 2019) and

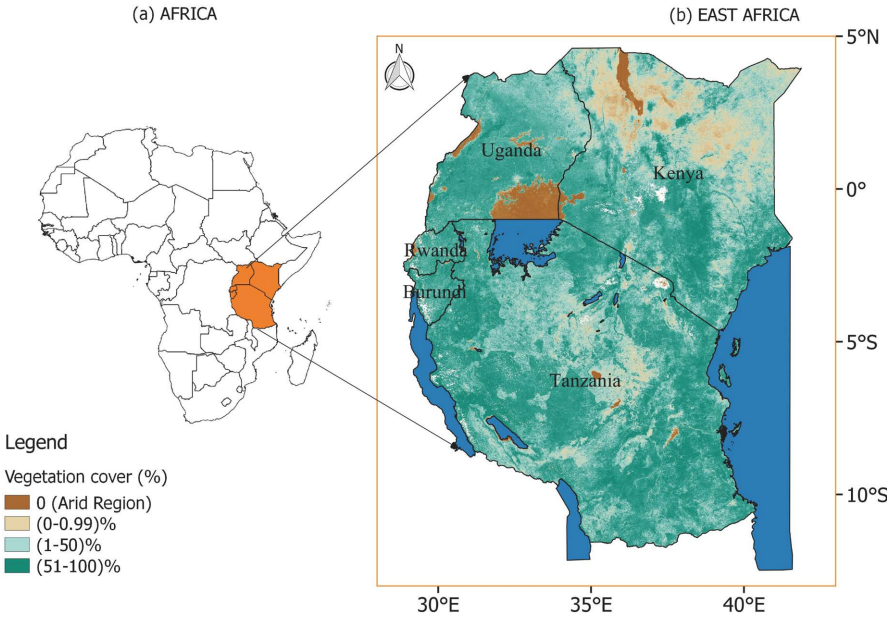

Figure 1. East Africa area showing the vegetation cover in percentage.

(Chang'a et al., 2017) in Tanzania. The geographical area comprises a variety of vegetative classifications, including grassland, forest, and agricultural land. These ecological systems play a significant role in enhancing biodiversity and sustaining ecological equilibrium.

2.2. Dataset

The monthly data that are used in this study have been collected over a period of time from 1983 to 2022. The main dataset used in this research is the NDVI, a widely used satellite derived metric that serves as an indicator of vegetation vitality and productivity. NDVI is derived from vegetation reflectance values in the red and near infrared (NIR) spectral bands, with the characteristic that healthy vegetation has a greater absorption of red light while reflecting a higher proportion of NIR (Kraetzig, 2022).

This research uses NDVI data from the Global Inventory Modelling and Mapping Studies, 3rd Generation V1.2 (GIMMS-3G+) dataset. The GIMMS-3G+ dataset provides an extensive temporal range of global NDVI data based on calibrated and adjusted measurements from the Advanced Very High-Resolution Radiometer (AVHRR) onboard various National Oceanic and Atmospheric Administration (NOAA) satellites. The spatial resolution of the dataset is 0.0833 degrees (approximately 8 km). The GIMMS-3G+ dataset implements corrections for numerous sources of data distortion, including calibration degradation, orbital drift, and environmental effects such as volcanic activity. These corrections demonstrate the integrity and reliability of the dataset for long-term vegetation monitoring. For the purposes of this research, the NDVI data has been extracted in NetCDF format to enhance the capacity for scientific investigation. By using this dataset, the study achieves a superior level of precision and uniformity in assessing interannual vegetation variability within EA, particularly in establishing correlations between NDVI variability and climatic factors as well as large-scale phenomena such as ENSO, IOD and AMO. The datasets have been obtained from the following link:

https://daac.ornl.gov/daacdata/global_vegetation/Global_Veg_Greenness_GIMMS_3G/data/.

The monthly mean sea surface temperature (SST) data were acquired from the National Oceanic and Atmospheric Administration (NOAA), exhibiting a latitude-longitude resolution of 2.0˚ × 2.0˚, which is accessible through the following link:

https://psl.noaa.gov/data/gridded/data.noaa.ersst.v5.html.

The Dipole Mode Index (DMI) is employed as a metric for the assessment of the Indian Ocean Dipole (IOD). The index is derived by calculating the differential between the mean sea surface temperature (SST) in the Western Indian Ocean, specifically within the coordinates of 50˚ - 70˚E and 10˚S - 10˚N, and the mean SST in the Eastern Indian Ocean, situated within the coordinates of 90˚E - 110˚E and 10˚S - 10˚N. The data utilized for this calculation is sourced from the Had-

ISST database. The data were obtained from the following link:

https://psl.noaa.gov/gcos_wgsp/Timeseries/Data/dmi.had.long.data.

The Niño 3.4 index plays an instrumental role in the analysis of the El Niño-Southern Oscillation (ENSO). This index has been constructed with the specific purpose of quantifying anomalies in SST within a defined region of the central Pacific Ocean. The Niño 3.4 region is bounded by latitudes between 5˚S and 5˚N and longitudes between 120˚W and 170˚W, as derived from HadISST data. The data can be accessed via the following link:

https://psl.noaa.gov/gcos_wgsp/Timeseries/Data/nino34.long.anom.data.

The study analyzes several key meteorological variables that are important for understanding climate and environmental conditions. These variables include precipitation, and soil moisture, which influences plant growth and ecosystem health. Moreover, the research investigates surface sensible heat flux and surface latent heat flux, essential for evaluating energy transfer between the land surface and the atmosphere. It also considers soil temperature at Level 1, which offers insights into soil thermal dynamics, alongside the temperature measured at 2 meters above ground to further assess atmospheric conditions and wind vectors.

The monthly mean precipitation data presented here have been obtained from the Climate Research Unit (CRU) at the University of East Anglia (Harris et al., 2020). This dataset is identified as version 4.07 (CRU TS 4.07) and has a horizontal resolution of 0.5˚ × 0.5˚; a link to download the data is provided:

https://crudata.uea.ac.uk/cru/data/hrg/cru_ts_4.07/cruts.2304141047.v4.07/pre/. CRU datasets have been used extensively in a wide range of scientific studies across the African continent. This dataset covers an extended temporal range and has been evaluated to determine its performance in relation to the Tanzanian context. The dataset has been used by (Koutsouris et al., 2016; Ongoma & Chen, 2017) to evaluate the variability of rainfall over the East African region. In addition, a number of scholars have employed this data set to examine the variability of precipitation within the same study area and it is therefore considered appropriate for the present study (Borhara et al., 2020).

The soil moisture dataset is obtained from the Climate Prediction Center (CPC) database, which has been carefully constructed by NOAA through the implementation of best interpolation techniques applied to quality assured gauge records derived from the Global Telecommunication System (GTS) framework. The spatial resolution of the datasets is 0.5˚ × 0.5˚ and can be accessed via the following link:

https://psl.noaa.gov/data/gridded/data.ncep.reanalysis.html.

However, monthly mean surface latent heat flux (SLHF), surface sensible heat flux (SSHF), soil temperature levels 1, 2m temperature. The data presented here have been obtained from the ERA5 database of the European Centre for Medium-Range Weather Forecasts (ECMWF), with a spatial resolution of 0.25˚ × 0.25˚, which can be accessed via the following link:

https://cds.climate.copernicus.eu/datasets/reanalysis-era5-single-levels-

monthly-means?tab=download.

Also, monthly mean Zonal and Meridional wind at 850 hPa with a resolution of 0.25˚ × 0.25˚ can be downloaded from this link:

https://cds.climate.copernicus.eu/datasets/reanalysis-era5-pressure-levels-monthly-means?tab=download.

2.3. Methodology

2.3.1. Standardized Anomaly

In this study, NDVI was subjected to a process of normalization in order to derive values corresponding to conditions of both wet and drought years. In particular, values corresponding to wet years were identified as exceeding +0.5, while those corresponding to drought years were characterised by measurements falling below −0.5. This approach allows for a more comprehensive understanding of vegetation health and moisture availability across different climatic regimes. This was accomplished by utilizing the following formula:

$$\textbf{\textit{Standardized Anomaly}} = \frac{\left(X - \bar{X}\right)}{\sigma} \tag{1}$$

In this equation, X represents the original value, $\bar{X}$ denotes the mean of the dataset, and σ (sigma) signifies the standard deviation of the dataset.

2.3.2. Statistically Significant Test

A student's t-test was employed to determine the statistical significance at the 95% confidence level. The two-sample t-test is an inferential statistical method that is employed to determine whether there is a significant difference between the means of two groups (Gore et al., 1977).

$$t = \frac{\overline{X_1} - \overline{X_2}}{\sqrt{\frac{\left[\left(N_1 - 1\right)S_1^2 + \left(N_2 - 1\right)S_2^2\right]\left(N_1 + N_2\right)}{\left(N_1 + N_2 + 2\right)\left(N_1 N_2\right)}}} \tag{2}$$

In this context, $\overline{X_1}$ and $\overline{X_2}$ represent the means of Sample 1 and Sample 2, respectively. Similarly, N_1 and N_2 denote the corresponding sample sizes, while S_1^2 and S_2^2 represent the standard deviations of Sample 1 and Sample 2, respectively.

2.3.3. Composite Analysis

A composite analysis utilizing the framework of conditional probability was conducted to investigate the relationship between the NDVI and various meteorological variables, as well as anomalies in sea surface temperature (SST). This analytical technique enabled the categorization of elevated NDVI values as indicative of wet years and diminished values as representative of drought years, in accordance with the framework established by (Aguilar et al., 2012; Areffian et al., 2021). By identifying and averaging selected variables associated with significant conditions (such as wet and drought years) derived from the NDVI, composite analysis enables comprehensive spatial mapping of vegetation health within defined climatic

contexts. This methodology is crucial for identifying areas significantly affected by atmospheric and oceanic influences, thereby facilitating a more profound comprehension of the interactions between climate and vegetation. Ultimately, composite analysis enhances the understanding of the effects of climate on vegetation dynamics within the study region.

2.3.4. Correlation Analysis

In the context of correlation analysis, a sample correlation coefficient is calculated, specifically the Pearson linear correlation coefficient (r). The sample correlation coefficient varies between −1 and +1. A value of −1 indicates a perfect negative correlation, whereby as one variable increases, the other decreases. Conversely, a value of +1 represents a perfect positive correlation, whereby as one variable increases, the other variable increases. A value of 0 signifies no correlation. The coefficient is employed to quantify both the direction and strength of the linear relationship that exists between the two variables. In this study, the Pearson correlation method was employed for the purpose of assessing the extent of the association between variables that exhibit a linear relationship (Clark et al., 2003; Habib et al., 2001).

$$r_{xy} = \frac{\sum_{i=1}^{n}\left(x_i - \bar{x}\right)\left(y_i - \bar{y}\right)}{\left(n-1\right)S_x S_y} \tag{3}$$

In this equation, the symbol r_{xy} represents the Pearson correlation coefficient, x_i this is the value of the variable x at the i[th] data point and y_i is the value of variable y at the i[th] data point, n represents the sample size, S_x this this is the standard deviation of the x values, S_y this is the standard deviation of the y values, which measures how spread out the values are from the average, $\bar{x}$ this is the average (mean) value of all x data points and $\bar{y}$ is the mean values of all y data points.

3. Results and Discussion

3.1. Spatiotemporal Variation of NDVI in East Africa

The examination of annual NDVI variability, as illustrated in **Figure 2(a)**, demonstrates significant fluctuations over temporal scales. In particular, high values of NDVI have been recorded in specific years, including 1998 and 2020, which achieved 0.53 and 0.52, respectively. These high NDVI values are presumably associated with favourable climatic conditions that facilitate vegetation growth, as evidenced by increased precipitation during El Niño events, which resulted in significant rainfall across East Africa during the 1997/1998 period. In contrast, years with reduced NDVI values, represented by 2009 and 2022 with respective values of 0.49 and 0.47, correspond to periods of low precipitation evidenced by (ASMET, 2019; IOM, 2023) or other unfavourable climatic conditions. Although a clear upward or downward trajectory is not evident across the entire period, this variability is indicative of the region's sensitivity to climate change and emphasizes the critical need for monitoring vegetative health in response to interannual

climatic variations.

This demonstrates how climatic fluctuations, driven by phenomena such as ENSO (El Niño-Southern Oscillation) and the Indian Ocean Dipole (IOD), impact NDVI metrics, thereby revealing both the ability of East Africa's ecosystems to withstand climatic alterations and their vulnerability to such changes. In years with higher precipitation levels, higher NDVI values are observed, whereas in years with lower precipitation levels, lower NDVI values are recorded. Furthermore, the interaction between NDVI variability and anomalies in sea surface temperature (SST) provides insight into a crucial relationship in understanding vegetation dynamics within the East African context. For instance, during episodes marked by the IOD, particularly in conjunction with El Niño events, a notable increase in precipitation is often observed, which can subsequently result in significantly higher NDVI values across the region (Kavishe & Limbu, 2020). Conversely, the occurrence of neutral or negative IOD phases is typically associated with reduced precipitation and diminished NDVI indices, thereby intensifying drought conditions and increasing the risk of food insecurity (Kavishe & Limbu, 2020).

On the spatial climatology of NDVI across East Africa showing the long-term distribution of vegetation across the region (**Figure 2(b)**), which is critical for identifying areas that may need targeted conservation efforts or sustainable land management practices, showing the annual average vegetation density across the region over the study period. The color scale ranges from red, indicating low NDVI (~0.2), to green, representing high NDVI (~0.6). Regions with high NDVI values, such as the southern part of Tanzania, the abundance of vegetation in this region is largely due to significant water bodies like Lake Nyasa (Lake Malawi). This large freshwater lake enhances local humidity and rainfall through evaporation, particularly during the austral summer rainy season, promoting vegetation growth along its banks (Diallo et al., 2018), also the Indian Ocean significantly influences southern Tanzania's climate and vegetation. Phenomena like ENSO and warm sea surface temperatures drive rainfall variability, enhancing precipitation and supporting vegetation growth in the region (Kim et al., 2021).

Uganda, Rwanda, Burundi, Western Tanzania also show high NDVI values, this is due to the proximity of water bodies over these areas such as the Lake Victoria Basin over Northern Tanzania and Lake Tanganyika over Western Tanzania and the Congo Basin over the western part of EA which bring more moisture over these areas to form more precipitation. In contrast, low NDVI areas, marked in red over most parts of Kenya and the North Eastern Highland of Tanzania as well as the central part, these areas are arid and semi-arid regions with little vegetation, these areas are characterized by minimal rainfall and high temperature.

The Standardized Anomaly was analyzed using NDVI data, employing the Equation (1) to achieve this objective. **Figure 3** provides crucial insights into the interannual fluctuations of vegetation within the region and demonstrates its

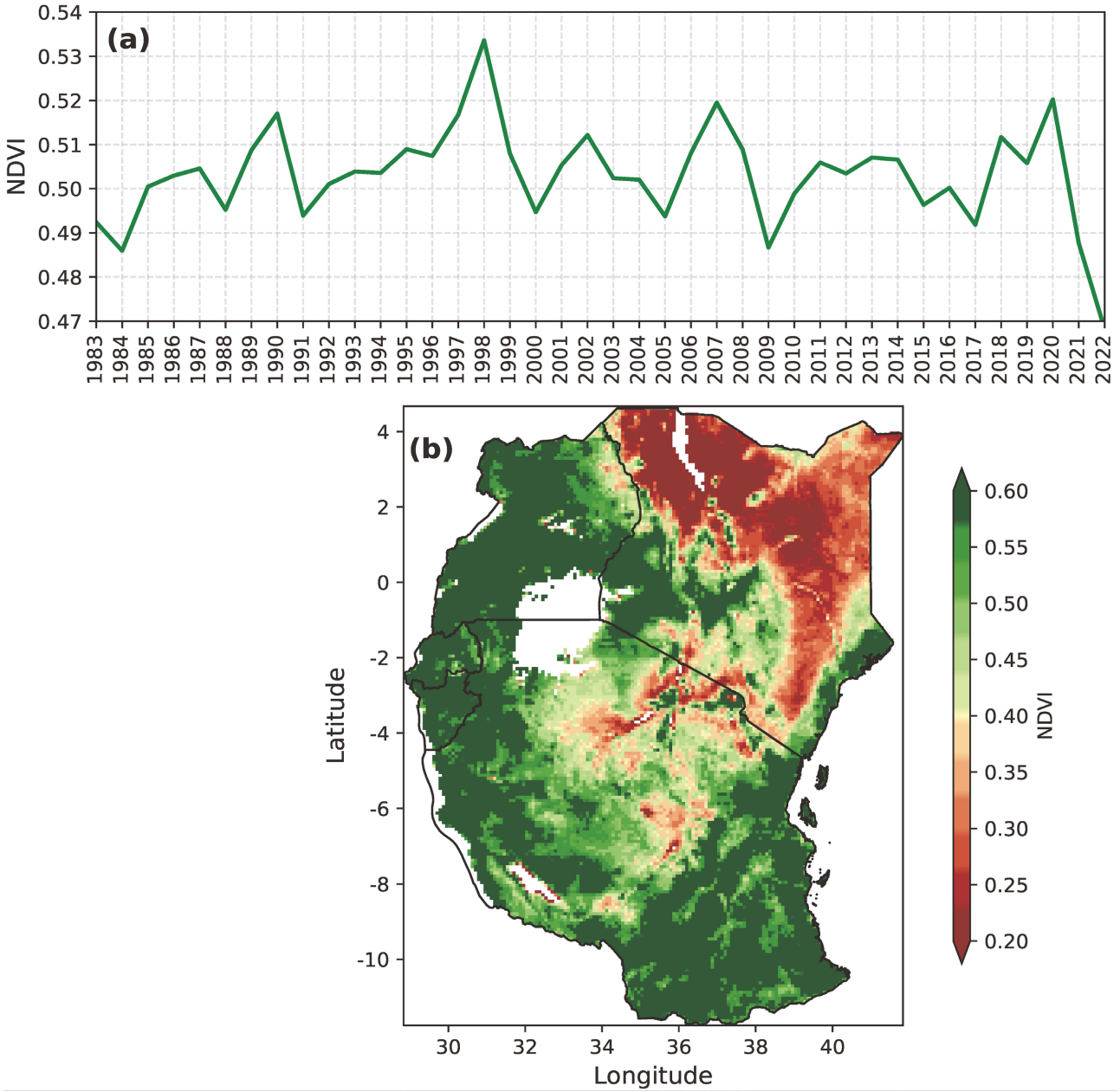

Figure 2. (a) illustrates the Annual mean time series of NDVI over East Africa from 1983 to 2022, and (b) the Annual mean spatial climatology of NDVI over East Africa.

responses to varying climatic conditions. By analyzing these fluctuations, it is possible to gain insight into the adaptive responses of vegetation in EA to periods of precipitation and drought over several decades. The black line represents the annual standardized NDVI anomaly values, which indicate periods of vegetative growth as well as decline. The red markers indicate wet years, defined as years with NDVI anomalies exceeding the threshold of +0.5, as marked by the red dotted line. The most notable wet year within this temporal series is 1998, which exhibits an extreme positive standardized anomaly linked primarily to the 1997/1998 ENSO events. The peaks indicate years during which conditions were conducive to vege-

tation growth, frequently correlated with above average precipitation levels. Such wet years are representative of periods of enhanced vegetation productivity, which is vital for both ecosystem functioning and agricultural output.

In contrast, green markers indicate dry years, during which NDVI anomalies decline below −0.5, as indicated by the blue dotted line. These years are typically characterised by unfavourable climatic conditions, such as drought, which have a negative impact on vegetation health and productivity. The value recorded in 2022, for instance, was particularly low, with much of EA experiencing below normal rainfall during that period. The occurrence of dry years indicates the region's vulnerability to water scarcity and environmental challenges, which can have a considerable impact on agriculture, water resources, and food security. The occurrence of wet and dry years is presented in (Table 1) for reference.

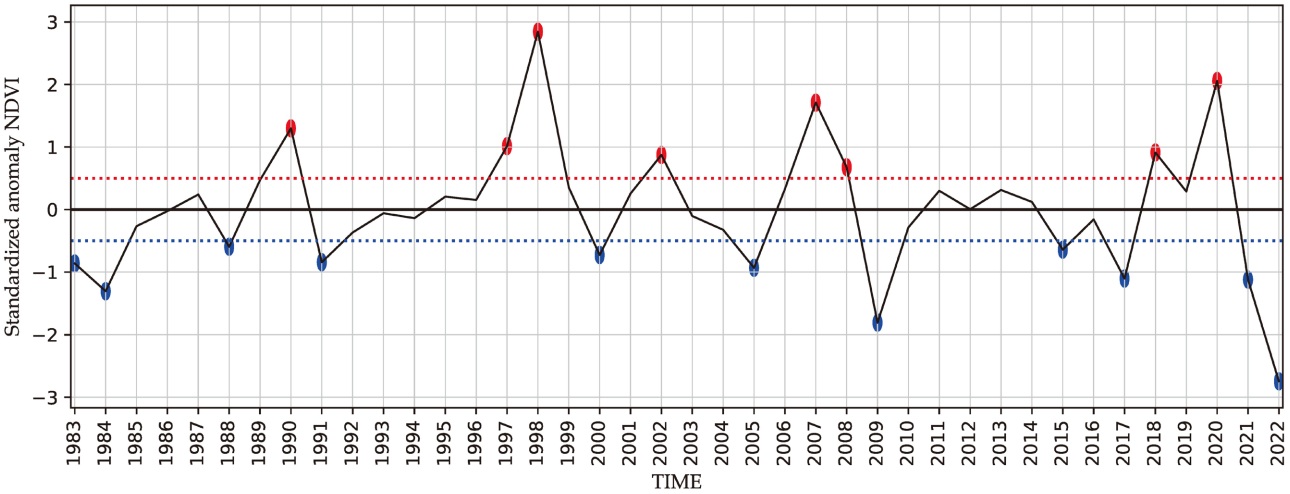

Figure 3. Shows the normalized NDVI over East Africa for the period 1983 to 2022, with years above 0.5 on the red dotted line representing wet years and years below 0.5 on the blue dotted line representing drought years.

Table 1. Illustrates the years in which there was an abundance of vegetation, categorized as wet years, and those in which there was a scarcity of vegetation, categorized as drought years.

Wet Years (8)	Drought Years (11)
1990, 1997, 1998, 2002, 2007, 2008, 2018, 2020	1983, 1984, 1988, 1991, 2000, 2005, 2009, 2015, 2017, 2021, 2022

3.2. Composite Analysis of NDVI and Associated Meteorological Variables and Oceanic Drivers

3.2.1. Composite Analysis of NDVI

Figure 4 presents a composite analysis of NDVI variability during wet and drought years across East Africa, along with the difference between these two extremes.

The spatial distribution of NDVI during wet years, which are characterised by widespread positive anomalies (Figure 4(a)). It is evident that the increased vegetation activity observed in these areas is likely driven by enhanced rainfall, which provides the necessary conditions for plant growth and improves vegeta-

tion cover. The regions exhibiting the highest NDVI values are Uganda, southern Kenya, western and southern Tanzania, and select areas of Rwanda and Burundi. This phenomenon can be attributed to the low incoming solar radiation experienced in these regions, which results in reduced evaporation and evapotranspiration (as indicated by low Surface Latent Heat Flux (SLHF) (**Figure 5(d)**). In contrast, high Surface sensible Heat Flux (SSHF) leads to greater outgoing solar radiation (**Figure 5(a)**), contributing to lower temperatures in these areas (**Figure 6(d)**), while moderate to high precipitation (**Figure 6(a)**) and soil moisture moderate to high (**Figure 7(a)**) are observed, alongside low soil temperatures (**Figure 7(d)**). Together, these interrelated factors have a collective impact on the elevation of NDVI values in these areas. These regions are more sensitive to favourable climatic conditions during wet years, as evidenced by their elevated NDVI values.

Despite experiencing wet years, certain regions displayed a decrease in NDVI values, particularly in most parts of Kenya and central and northeastern Tanzania. Meteorological variables contribute to this phenomenon, such as high SLHF in these areas (**Figure 5(d)**), which results in increased evaporation and evapotranspiration. Additionally, low SSHF (**Figure 5(a)**) indicates diminished outgoing solar radiation, leading to warmer surface temperatures (**Figure 6(d)**) and elevated soil temperatures (**Figure 7(d)**), which in turn result in reduced soil moisture (**Figure 7(a)**) and low precipitation levels in these regions (**Figure 6(a)**). Collectively, these conditions contribute to the observed decline in NDVI values in these areas (**Figure 4(a)**).

The NDVI composite for drought years characterised by a marked decrease in the health of vegetation in East Africa (**Figure 4(b)**). The reduction in NDVI values observed during periods of drought suggests a deterioration in vegetation health, predominantly caused by water scarcity and high temperatures. Notably, a decline in NDVI has been recorded in northern Kenya, as well as in the central and northeastern regions of Tanzania, where similar meteorological factors that influence wet years also impact drought years over the same region. The reduction in NDVI values is indicative of the vulnerability of East African ecosystems to drought conditions, given that the growth and productivity of vegetation are critically dependent on sufficient water availability.

Despite experiencing drought years, some regions, such as Uganda, Rwanda, Burundi, western and southern Tanzania, have shown an increase in NDVI values. This occurrence may be linked to climatic phenomena like El Niño and La Niña, which can produce intermittent rainfall even during drought conditions. Such intermittent rainfall may encourage short-term vegetative growth in certain resilient plant species; however, it is not enough to sustain the overall health of the ecosystem. Additionally, similar meteorological factors observed during wetter years in these areas contribute to the increase in vegetation.

The difference between NDVI composites for wet and drought years, highlighting the spatial variations (**Figure 4(c)**). A positive NDVI value indicates an increase

during wet years compared to drought years, thereby identifying regions that demonstrate enhanced responsiveness to favourable precipitation conditions and other meteorological conditions. In contrast, a negative NDVI value denotes a decrease in wet years relative to drought years, with declines observed across Uganda, Rwanda, Burundi, western and southern regions of Tanzania. Key meteorological factors contributing to this decline include high SLHF over these areas (Figure 5(f)), which leads to increased evaporation and evapotranspiration, and low SSHF (Figure 5(c)), indicating reduced outgoing solar radiation. This combination results in warmer surface temperatures (Figure 6(f)) and elevated soil temperatures (Figure 7(f)), which ultimately cause lower soil moisture levels (Figure 7(c)). Additionally, precipitation levels in these regions are low (Figure 6(c)), intensifying the conditions that lead to a reduction in NDVI values (Figure 4(c)). This serves to illustrate that these regions are particularly vulnerable to the effects of drought. This is due to the fact that, in comparison to the drought years, there was minimal vegetation during the wet years in these areas.

Conversely, a notable increase in vegetation was recorded in the central and northeastern parts of Tanzania and in significant portions of Kenya. This is due to the fact that there were greater NDVI values during the wet years than in the drought years over these areas. The figure provides vital insight into the regions of East Africa that are most severely affected by climatic variability. The meteorological factors influencing this phenomenon include low incoming solar radiation in these areas, which results in reduced evaporation and evapotranspiration (indicated by low SLHF) (Figure 5(f)). Additionally, high SSHF leads to increased outgoing solar radiation (Figure 5(c)), which contributes to lower temperatures in these regions (Figure 6(f)), alongside moderate to high precipitation (Figure 6(c)) and moderate to high soil moisture (Figure 7(c)). Furthermore, low soil

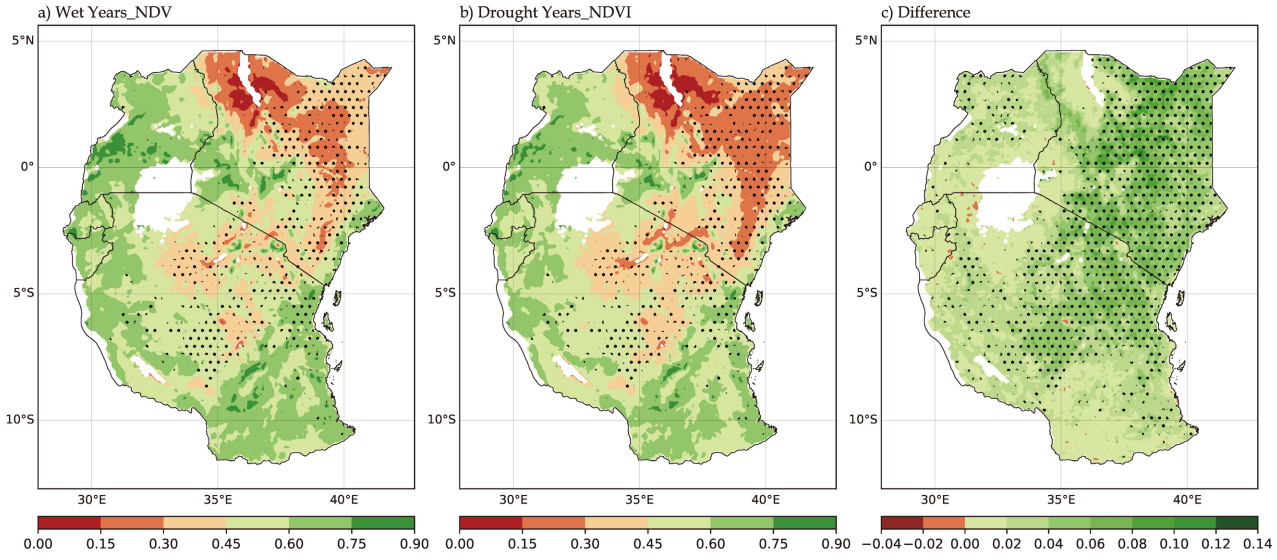

Figure 4. Illustrates the following: (a) a composite analysis of NDVI during a wet year, (b) a composite analysis of NDVI during a dry year, and (c) the difference between the composite of the wet year and the dry year. The black dots indicate areas where statistically significant change have occurred at the 95% confidence level.

temperatures (Figure 7(f)) also play a role in this dynamic. Collectively, these factors have contributed to the rise in NDVI values across these areas (Figure 4(c)).

The presence of black dots on the maps indicates statistically significant changes at the 95% confidence threshold, thereby indicating areas where vegetation's response to climate variability is particularly pronounced.

3.2.2. Composite Analysis of Meteorological Variables

This section presents the results of a composite analysis exploring the influence of key meteorological variables on the variability of NDVI over East Africa. The analysis considers the impact of Surface Sensible Heat Flux (SSHF), Surface Latent Heat Flux (SLHF), precipitation, temperature, soil moisture and soil temperature.

1) Composite Analysis of SSHF and SLHF

As illustrated in Figure 5(a), the SSHF is presented as a composite during the wet years. SSHF represents a quantitative measure of the transfer of thermal energy from the terrestrial surface to the atmosphere, occurring through the mechanisms of conduction and convection. The majority of East African regions exhibit moderate SSHF, while low SSHF is observed over northern Kenya and small areas of north-eastern Tanzania. Furthermore, the region experienced elevated SLHF (Figure 5(d)), which resulted in elevated temperatures (Figure 6(d)) due to the excess of incoming solar radiation over outgoing solar radiation. The occurrence of high SLHF results in elevated evaporation rates, which in turn lead to a reduction in soil moisture (Figure 7(a)) and an increase in soil temperature (Figure 7(d)). In consequence of these conditions, precipitation levels were low (Figure 6(a)), which in turn resulted in low NDVI values (Figure 4(a)).

The elevated SSHF observed over water bodies, such as Lake Turkana in Kenya and Lakes Victoria and Tanganyika in Tanzania, can be attributed to the specific thermal properties of water, in contrast to land, water is capable of absorbing a considerable quantity of heat with only a slight increase in temperature. During daylight hours, lakes effectively absorb heat from solar radiation and subsequently release it back to the atmosphere as sensible heat. This process is responsible for the elevated SSHF, particularly during periods of temperature change.

As demonstrated in Figure 5(b), a composite of SSHF during the drought years exhibits a pattern that is largely similar to that observed during the wet years. However, it demonstrates an increase in the area of low SSHF over Kenya and northeastern Tanzania.

The findings suggest that across the majority of Kenya and northeastern Tanzania, there is a high prevalence of SSHF (Figure 5(c)). This suggests that during periods of wet years, these regions exhibited a significant prevalence of SSHF. Furthermore, the region exhibits a minimal level of SLHF (Figure 5(f)). This is accompanied by a low temperature (Figure 6(f)), low soil temperature (Figure 7(f)), high soil moisture (Figure 7(c)), and moderate precipitation (Figure 6(c)). In summary, these conditions have resulted in an increase in NDVI values (Figure

4(c)) in these areas. In contrast, the result indicates Lake Victoria basin, western and southern Tanzania show low prevalence of SSHF (Figure 5(c)), accompanied by a high prevalence of SLHF (Figure 5(f)). This results in elevated temperatures (Figure 6(f)), high soil temperatures (Figure 7(f)), low soil moisture (Figure 7(c)), and low precipitation (Figure 6(c)), which collectively lead to low NDVI values (Figure 4(c)) in these areas.

The composite of SLHF during the wet years is illustrated in Figure 5(d). Elevated SLHF values indicate increased latent heat release due to higher surface humidity and increased evaporation, often driven by incoming solar radiation. In particular, higher SLHF values are observed in northern Kenya, suggesting that regions with elevated SLHF may experience significant rainfall due to atmospheric moisture accumulation. However, given the arid to semi-arid nature of this area, the effects of high SLHF lead to soil drying (Figure 7(a)), especially when rainfall is insufficient (Figure 6(a)) to restore soil moisture. In contrast, the remaining regions have moderate SLHF values, indicating a balance between evaporation and evapotranspiration, driven by moderate incoming solar radiation, which increases the availability of moisture in the atmosphere. Under favourable conditions, such as sufficient heat and atmospheric instability, this increased moisture supports cloud formation and precipitation (Figure 6(a)). Very low SLHF is observed over the water bodies of Lake Turkana in Kenya, Lake Victoria and Tanganyika in Tanzania, because water has a high specific heat capacity, meaning it can absorb and store large amounts of heat without a significant change in temperature. This property allows water to moderate temperature fluctuations more effectively than land, which can lead to differences in SLHF (Figure 5(d)).

The composite of SLHF during drought years is shown in (Figure 5(e)). Higher SLHF values indicate a greater amount of incoming solar radiation over the area, which can be observed in northern and eastern Kenya and parts of northeastern and central Tanzania; during the drought year, the area of high SLHF has increased, causing more evaporation and evapotranspiration, resulting in stress on the vegetation (Figure 4(b)). In contrast, the remaining areas have moderate SLHF.

The composite difference in SLHF between wet and drought years is illustrated in (Figure 5(f)). The results demonstrate that the Lake Victoria basin, along with the regions of Western and Southern Tanzania, display high SLHF values, indicating that these areas have experienced high SLHF during periods wet years. In contrast, the analysis indicates that low SLHF values are present over Kenya and north-eastern Tanzania, which suggests that in these areas, SLHF was higher during drought years. This pattern suggests that greater quantities of moisture are being evaporated from the surface during drought periods, which may result in the drying out of soils (Figure 7(c)) and vegetation (Figure 4(c)). During droughts, soil moisture is already limited, thus increased evaporation can lead to further water scarcity.

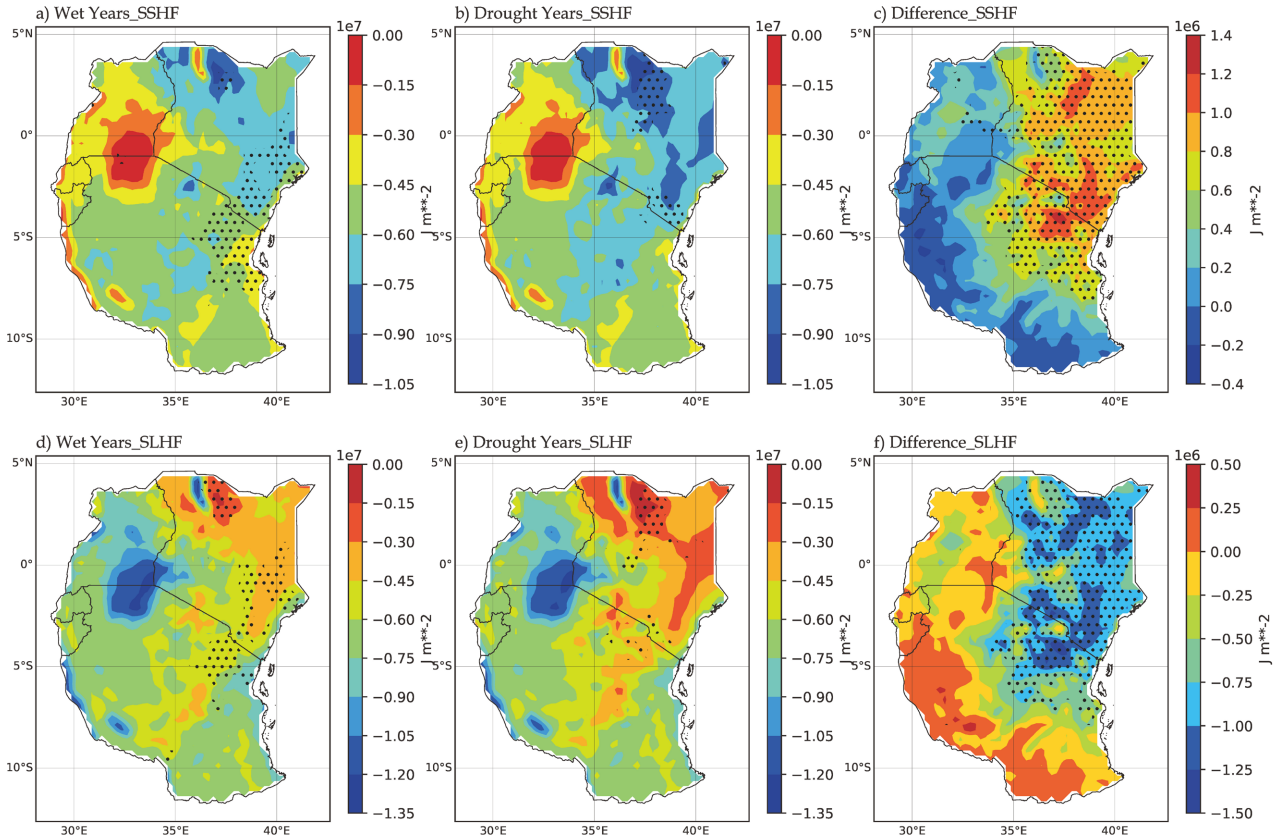

Figure 5. Shows the composite of surface sensible heat flux (SSHF) and surface latent heat flux (SLHF) during three different climatic periods: (a) wet years for SSHF, (b) dry years for SSHF and (c) the difference between wet and drought years for SSHF (d)) wet years for SLHF (e) dry years for SLHF and (f) the difference between wet and drought years for SLHF. Black dots indicate areas where statistically significant changes have occurred at the 95% confidence level

2) Composite Analysis of Precipitation and 2m Temperature

Figure 6(a) illustrates the composite precipitation patterns observed during the wet years. Despite the overall wet years, some areas have experienced low precipitation, as evidenced by observations across the majority of Kenya, central and northeastern Tanzania. This region displays a combination of elevated SLHF (Figure 5(d)) and reduced SSHF (Figure 5(a)), which results in elevated temperatures (Figure 6(d)). These conditions contribute to a reduction in precipitation, as illustrated in (Figure 6(a)). The region is prone to drought conditions, as high evaporation rates may intensify water deficits even when atmospheric humidity is considerable, thereby limiting precipitation. Regions that experience lower rainfall even during wet years are often more prone to drought conditions, which can intensify food insecurity and exert a significant burden on local economies (Kalisa et al., 2021). Although precipitation levels were high in some areas of the Lake Victoria basin, in Western Kenya and in some parts of southern Tanzania (Figure 6(a)), the high SSHF observed over this region (Figure 5(a)) and the low SLHF (Figure 5(d)) resulted in low temperatures (Figure 6(d)), creating an environment conducive to rainfall in these areas.

As illustrated in Figure 6(b), composite precipitation patterns were observed

during the drought years. This illustrates a widespread reduction in precipitation, with the areas that were previously characterised by high precipitation from the composite of wet years now largely absent. This suggests that precipitation levels across East Africa were significantly reduced during periods of drought. The majority of Kenya, central and northeastern regions of Tanzania exhibited low precipitation levels. These areas are prone to drought, which increases the risk of water scarcity, crop failure and environmental stress (Kijazi & Reason, 2009).

However, the areas surrounding the Lake Victoria Basin exhibited an increase in precipitation during the drought years. This phenomenon can be attributed to the presence of low SLHF in this region (**Figure 5(e)**), coupled with high SSHF (**Figure 5(b)**), which resulted in a decline in temperature across the area (**Figure 6(e)**). Collectively, these climatic conditions contributed to an enhanced precipitation rate (**Figure 6(b)**). The lake serves as a climatic regulator, affecting local weather systems and, in turn, precipitation levels in adjacent regions.

The composite difference in precipitation between wet and drought years is shown in (**Figure 6(c)**). The results demonstrate that majority of areas in Kenya, Uganda, Rwanda, Burundi, and select regions in the southern part of Tanzania, exhibited low precipitation levels. Indicating that during wet years these areas received less precipitation in comparison to drought years. The Indian Ocean Dipole (IOD) has a more pronounced effect on precipitation patterns in Tanzania than other modes of variability (Borhara et al., 2020). During periods of negative oscillation, there is a notable reduction in rainfall in southern Tanzania, which in turn leads to drier conditions. The intertropical convergence zone (ITCZ), which varies its location in accordance with seasonal thermal dynamics, has the potential to induce anomalous rainfall distributions during periods of drought (Palmer et al., 2023). The presence of mountain ranges or elevated terrain can facilitate orographic lifting, whereby moist air is forced to ascend and undergo cooling and condensation, ultimately resulting in precipitation. This phenomenon can be observed in regions adjacent to the Great Rift Valley, as well as in the elevated terrain of Kenya and Uganda, where enhanced rainfall due to orographic influences has been documented even during periods of broader drought conditions (Borhara et al., 2020; Palmer et al., 2023).

The western, central, north eastern and eastern parts of Tanzania exhibit moderate to high rainfall (**Figure 6(c)**), indicating that these areas received more precipitation during the wetter years compared to drought years. This may be the cause of the observed increase in vegetation in these areas, as illustrated in **Figure 4(c)**. During wetter years, these areas are able to benefit from the moisture levels that are conducive to the growth of a variety of plant species. As illustrated in **Figure 7(c)**, elevated precipitation levels lead to enhanced soil moisture, which helps vegetation to flourish.

The 2-meter temperature composite during the wet years is illustrated in **Figure 6(d)**. The results indicate that during wet years, temperatures are typically

lower over some areas in East Africa, particularly in the southern region of Kenya, the Northeastern and in some areas South Tanzania and Northern Rwanda. The elevated precipitation levels (**Figure 6(a)**) are associated with increased cloud cover, which contributes to a reduction in surface heating, as illustrated in **Figure 5(d)**. This is due to the fact that clouds reflect sunlight and limit solar radiation from reaching the Earth's surface directly which leads to low temperature over these areas.

The highest temperatures are being recorded in the northern regions of the East African, with the most significant increases observed in northern and eastern Kenya. Over this region High SLHF (**Figure 5(d)**) is observed which causes more incoming solar radiation and Low SSHF (**Figure 5(a)**) causes low outgoing long wave radiation this causes warming over this area (**Figure 6(d)**). A significant increase in temperature from December to February is attributable to the prevailing winds, which originate from the land and frequently transport heat into the region (Gilbert Ouma, 2024). Furthermore, the long-term effects of climate change have resulted in an increase in mean annual temperatures, leading to elevated conditions throughout historically humid months (Gilbert Ouma, 2024).

Figure 6(e) illustrates the 2-meter temperature composite during the Drought years, show almost similar pattern to wet years, but here the area of high temperature over North and Eastern Kenya as increased.

The composite difference in 2-metre temperature between wet and drought years is shown in **Figure 6(f)**. The results demonstrate that high temperatures were observed over Uganda, Rwanda, Burundi, the western and southern regions of Tanzania. This shows during the wet years these areas had high temperature compared to drought years. These areas are dominated by high SLHF (**Figure 5(f)**) and low SSHF (**Figure 5(c)**) which make these areas warmer (**Figure 6(f)**). The elevated temperatures during periods of wet years can induce stress in plant systems despite the presence of adequate moisture levels as illustrated in **Figure 4(c)**.

In the context of high temperature regimes, transpiration rates tend to increase, reflecting a rise in the rate at which plants expel water through their leaves. When temperatures increase significantly, the equilibrium between water absorption by root systems and water loss through transpiration may be disrupted, resulting in a scenario where plants may experience water stress despite the presence of sufficient soil moisture (Fu et al., 2024). The result over central and northeastern regions of Tanzania as well as northern area of Kenya show low temperature, these same regions experienced high temperatures during the drought years and low temperature during wet years. Lower ambient temperatures typically enhance the water use efficiency of flora, as they diminish the rates of evaporation occurring within the soil. This phenomenon enables plants to sustain their hydration levels during critical phases of development, thereby promoting increased growth rates and biomass density as illustrated in **Figure 4(c)**.

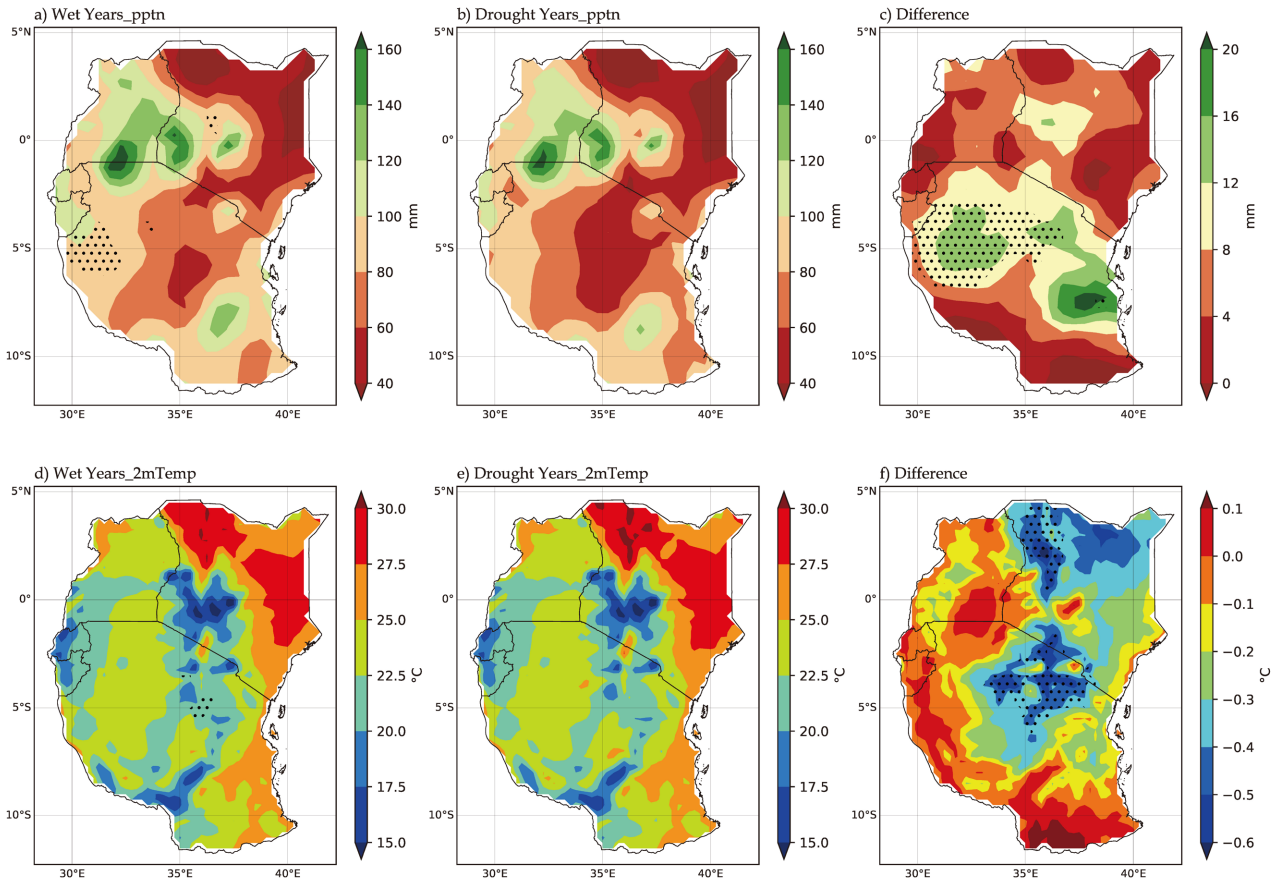

Figure 6. Shows the composite of Precipitation and Temperature during three different climatic periods: (a) wet years for Precipitation, (b) dry years for Precipitation and (c) the difference between wet and drought years for precipitation (d) wet years for 2m temperature (e) dry years for 2m temperature and (f) the difference between wet and drought years for 2m temperature. Black dots indicate areas where statistically significant changes have occurred at the 95% confidence level.

3) Composite Analysis of Soil Moisture and Soil Temperature

The composite of soil moisture during the wet years is illustrated in **Figure 7(a)**. The results demonstrate that the most areas of Tanzania exhibit moderate soil moisture, while the Lake Victoria basin and Western Kenya display high soil moisture observed, due to elevated precipitation levels (**Figure 6(a)**), low soil temperature (**Figure 7(d)**), low air temperature over these areas (**Figure 6(d)**), low SLHF (**Figure 5(d)**) and high SSHF (**Figure 5(a)**). Conversely, the north and east of Kenya exhibit low soil moisture, which can be attributed to reduced precipitation in these regions, as illustrated by **Figure 6(a)**, high SLHF (**Figure 5(d)**) and low SSHF (**Figure 5(a)**) resulted into high temperature (**Figure 6(d)**).

A reduction in soil moisture levels results in stress in vegetation due to the restriction of the water necessary for vital processes, including those related to photosynthesis and respiration. In the event of inadequate soil moisture levels, plants are unable to absorb an adequate volume of water through their root systems, resulting in a deficiency in the essential hydration required for optimal growth and development. Furthermore, reduced soil moisture levels result in the restriction of nutrient transport within the plant structure. The transport of nutrients from

the soil into the plant roots is dependent on the presence of water.

Figure 7(b) illustrates the composite of soil moisture during the drought years, demonstrating comparable outcomes to those observed during the wet years. Nevertheless, it is notable that the area exhibiting low soil moisture has increased, while the area displaying high soil moisture has diminished.

The composite difference in soil moisture between wet and drought years is illustrated in Figure 7(c). The results show that most regions of Kenya and northeastern Tanzania have elevated soil moisture, which is conducive to plant growth (Figure 4(c)). In addition, the soil temperature in these regions is relatively low (Figure 7(f)), which is a consequence of the high SSHF (Figure 5(c)) and low SLHF (Figure 5(f)). This results in low temperatures over these areas (Figure 6(f)) and moderate rainfall (Figure 6(c)). These factors contribute to an increase in soil moisture in this region. The observed decrease in soil moisture was attributable to the confluence of elevated SLHF (Figure 5(f)) and diminished SSHF (Figure 5(c)) over the regions of western Uganda, Rwanda, Burundi, western and southern Tanzania. These conditions gave rise to elevated temperatures (Figure 6(f)), and decrease in NDVI value in these areas (Figure 4(c)).

The soil temperature employed in this study corresponds to level 1, which represents a depth range of 0 to 7 cm. Figure 7(d) presents a composite of soil temperature during the wet years. The results indicate that elevated soil temperatures are observed in northern and eastern Kenya. It is evident that such temperatures have the potential to exert a negative influence on the growth and development of numerous plant species in this region, as illustrated in Figure 4(a). The elevated soil temperatures observed in this region can be attributed to a combination of factors, including high SLHF (Figure 5(d)) and low SSHF (Figure 5(a)). These conditions have resulted in a rise in temperature across these areas (Figure 6(d)) and a reduction in precipitation (Figure 6(a)). Elevated soil temperatures have been demonstrated to enhance the viscosity of water, thereby reducing its uptake by plant roots and subsequently decelerating the movement of nutrients (Pregitzer & King, 2005).

Additionally, the findings suggest that the reduced soil temperatures observed in southern Kenya are influenced by diminished SLHF (Figure 5(d)) and elevated SSHF (Figure 5(a)), which subsequently resulted in lower temperatures (Figure 6(d)) and increased precipitation (Figure 6(a)) in this region. The remaining area exhibits moderate soil temperatures.

The composite of soil temperature during the drought years is shown in Figure 7(e). The results demonstrate that soil temperatures during drought years are higher, particularly in the northern and eastern regions of Kenya. This is due to a reduction in rainfall (Figure 6(b)) and less cloud cover during drought years, which allows for more direct solar radiation to heat the soil (Figure 5(e)), leading to higher surface temperatures (Figure 6(e). The high soil temperatures observed during drought years can intensify the stress experienced by vegetation, as plants contend with the combined effects of elevated temperatures and water scarcity.

A decline in soil temperature has been documented in Rwanda, Burundi, south-

ern Tanzania, and southern Kenya. This decline is associated with increased precipitation over the region (Figure 6(b)), higher soil moisture levels (Figure 7(b)), reduced incoming solar radiation, indicated by low SLHF (Figure 5(e)), and increased outgoing solar radiation, reflected by high SSHF (Figure 5(b)). These conditions have collectively contributed to lower overall temperatures in the region (Figure 6(e)), creating a favorable environment for vegetation growth (Figure 4(b)).

The composite difference in soil temperature between wet and drought years is illustrated in Figure 7(f). The results indicate that regions including Uganda, Rwanda, Burundi, the Lake Victoria basin, and western and southern Tanzania exhibit elevated soil temperatures, suggesting that during wet years, these areas experienced higher soil temperatures compared to drought years. The elevated soil temperatures can likely be attributed to higher air temperatures (Figure 6(f)), which often correlate with increased solar radiation (i.e., high SLHF; (Figure 5(f)), reduced outgoing solar radiation (i.e., low SSHF; (Figure 5(c)), and decreased precipitation (Figure 6(c)). These conditions not only result in a decline in

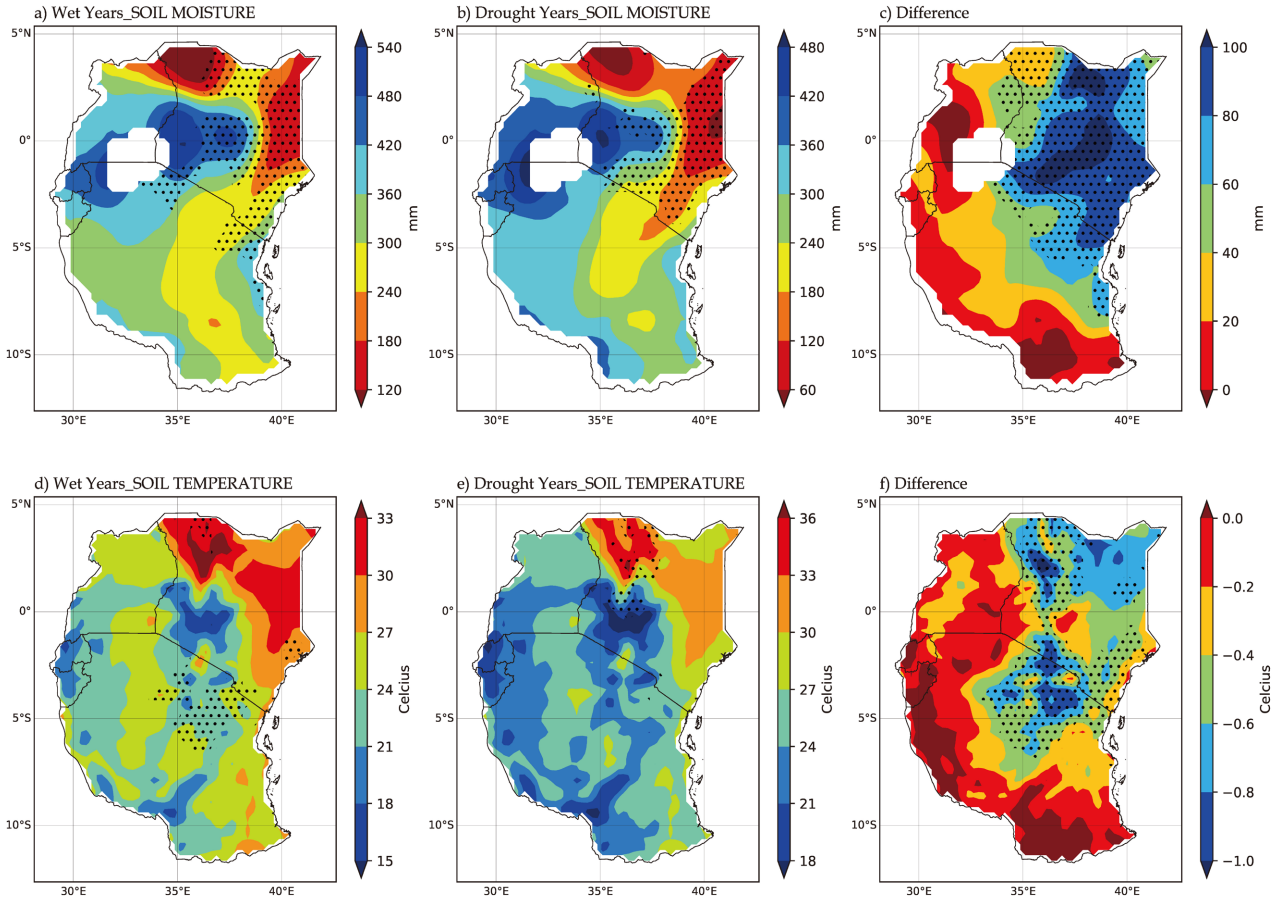

Figure 7. Shows the composite of Soil Moisture and Soil Temperature at level 1 {depth 0~7cm) during three different climatic periods: (a) wet years for Soil Moisture, (b) dry years for Soil Moisture and (c) the difference between wet and drought years for Soil Moisture (d) wet years for Soil temperature (e) dry years for Soil temperature and (f) the difference between wet and drought years for Soil temperature. Black dots indicate areas where statistically significant changes have occurred at the 95% confidence level.

vegetation in the region (Figure 4(c)), but also lead to a reduction in the soil's capacity to retain moisture (Figure 7(c)), thereby intensifying the effects of drought during periods of low precipitation (Figure 6(c)).

The results also indicate the presence of regions exhibiting low soil temperatures, including the majority of areas within Kenya and the northeastern region of Tanzania. The low soil temperatures are influenced by two factors: reduced incoming solar radiation, which is reflected in the low SLHF (Figure 5(f)), and increased outgoing solar radiation, indicated by the high SSHF (Figure 5(c)). These factors contributed to a reduction in air temperature in the region (Figure 6(f)), moderate precipitation levels (Figure 6(c)), and elevated soil moisture (Figure 7(c)). In sum, these conditions created a favourable environment for vegetation growth in this area (Figure 4(c)).

3.2.3. Composite Analysis of Oceanic Drivers

SST and Wind circulations during wet years are shown in Figure 8(a), the equatorial Pacific and North Atlantic regions show warmer SST anomalies; this phenomenon is likely to be a consequence of enhanced upwelling and increased heat exchange with the atmosphere, which subsequently favours increased evaporation. This process leads to an increased concentration of moisture in the atmosphere, facilitating precipitation when this moisture is transported to East Africa. Conversely, the Southern Ocean and certain sectors of the North Pacific have cooler temperatures due to increased oceanic heat uptake and the presence of strong westerly winds.

Figure 8(b) Conversely, periods of drought are characterised by an observable warming trend in the Southern Ocean and certain regions of the North Pacific, while the Equatorial Pacific and North Atlantic show lower sea surface temperatures (SSTs) and reduced trade winds.

The composite difference in SSTs and wind circulations during periods of wet years and those characterised by drought years is illustrated in Figure 8(c); the most pronounced differences are seen in the equatorial Pacific and the Southern Ocean. Wind vectors show a marked weakening of the trade winds, which tends to modify the atmospheric circulation patterns that affect the distribution of precipitation during drought years, particularly in the equatorial Pacific. This weakening is likely to be a major factor driving the observed changes in SST. An important phenomenon correlated with trade winds is the ENSO, which includes

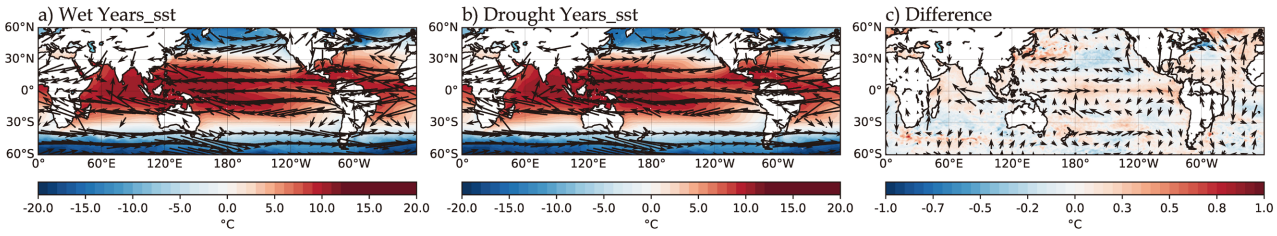

Figure 8. Spatial Sea Surface Temperature (SST) composite with overlayed wind data at 850 hPa during (a) wet years, (b) drought years, and (c) the difference between the wet years and Drought years.

both the El Niño and La Niña phases. Reduced trade winds can intensify El Niño events, generally leading to increased rainfall in certain regions of East Africa, while La Niña can lead to reduced rainfall.

3.3. Correlation Analysis

Figure 9 presents the spatial distribution of annual correlation coefficients between NDVI and six Meteorological variables over East Africa from 1983 to 2022.

A predominantly significant negative correlation between NDVI and SLHF (Figure 9(a)) is observed in most regions, particularly in northern EA, where increased SLHF (Figure 5(d) and Figure 5(e)) correlates with decreased NDVI (Figure 4(a) and Figure 4(b)), probably due to water loss from soil and vegetation caused by higher surface evaporation. However, there is a positive, although not statistically significant, correlation in parts of western and southern Tanzania, where sufficient moisture and energy may promote vegetation growth. Conversely, NDVI shows a significant positive correlation with SSHF across most of EA (Figure 9(b)), as higher SSHF (Figure 5(c)) is likely to improve soil temperature, nutrient availability and biological activity, thereby promoting vegetation growth (Figure 4(c)) over the northern part of EA. Precipitation also shows a strong positive correlation with NDVI (Figure 9(c)), especially in central EA, where increased precipitation (Figure 6(c)) corresponds to healthier vegetation, while areas with less precipitation show reduced vegetation health (Figure 4(c)).

NDVI shows a predominantly negative correlation with 2m temperature (Figure 9(d)) and soil temperature (Figure 9(e)), especially in the northern EA, where increasing temperatures (Figure 6(d) and (Figure 6(e)) correspond to reduced NDVI (Figure 4(a) and Figure 4(b)), suggesting stress on vegetation health. In contrast, soil moisture has a strong positive correlation with NDVI across the EA (Figure 9(f)), with significant effects in northern EA, where increased soil moisture (Figure 7(c)) is associated with improved vegetation health (Figure 4(c)), highlighting its critical role in maintaining vegetation, particularly in regions with unique climatic or geological conditions.

The annual correlation between the standardized anomalies of NDVI and three climatic indices: the Dipole Mode Index (DMI), the Nino 3.4 Index, and the Atlantic Multidecadal Oscillation (AMO), the data set spans the period from 1983 to 2022 (Figure 10).

A weak positive correlation between NDVI and the Dipole Mode Index (DMI) ($r = 0.11$) is illustrated in Figure 10(a), indicating that the IOD exerts a limited direct influence on NDVI variability in the region. Although some synchronized patterns between NDVI and DMI are observed, it is likely that other factors, such as precipitation, temperature and local environmental conditions, play a more substantial role in shaping vegetation dynamics. It is notable that the combined effects of DMI and the Nino 3.4 Index illustrate the importance of considering multiple climatic factors, as their interaction may exert a significant influence on

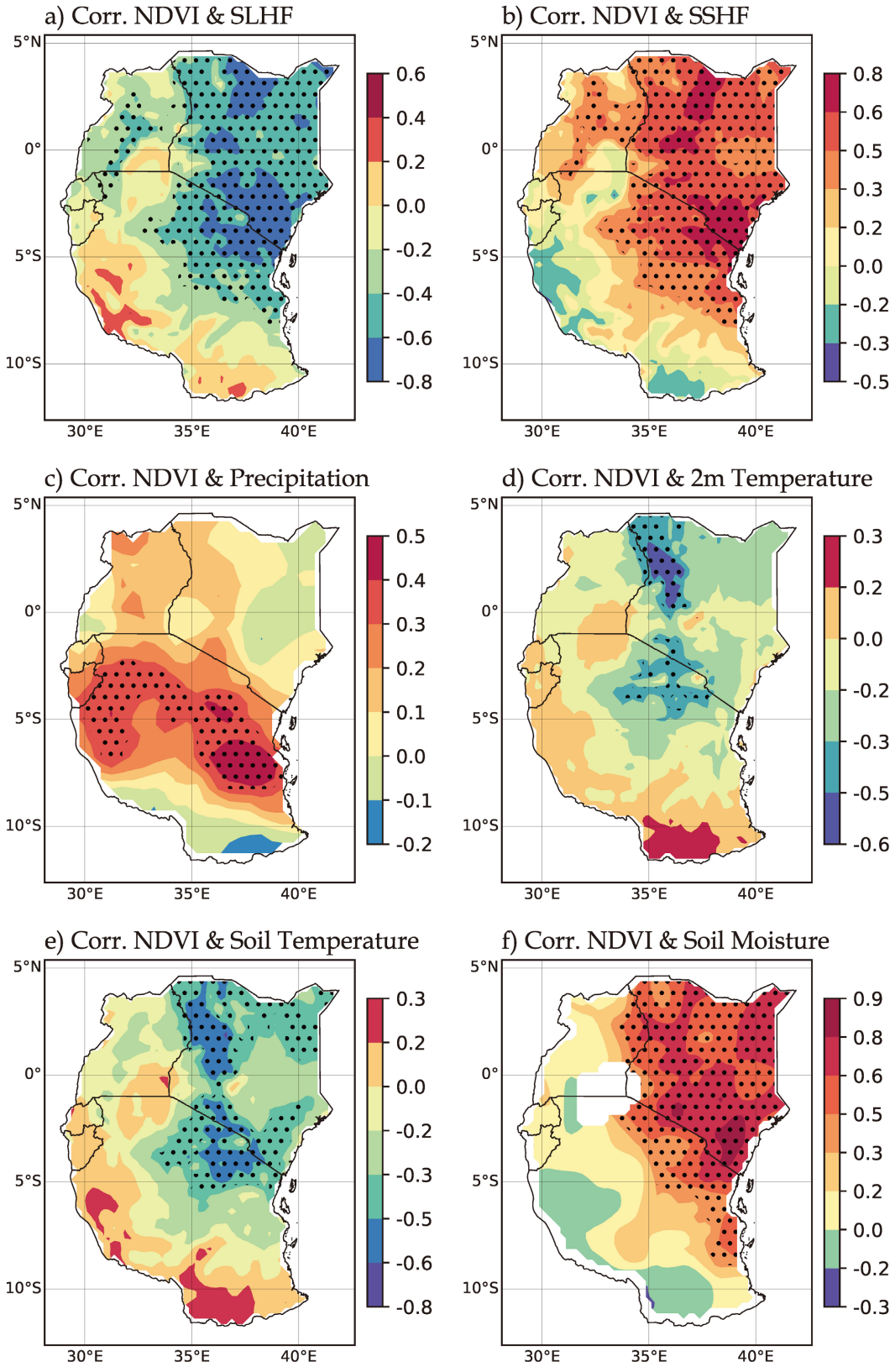

Figure 9. Illustrates the annual correlation between Normalized NDVI and (a) SLHF, (b) SSHF, (c) Precipitation, (d) 2m temperature, (e) Soil temperature, and (f) Soil moisture over the period 1983 to 2022. statistically significant areas at the 95% confidence level are marked with black dots.

vegetation growth and health.

A moderate positive correlation between NDVI and the Nino 3.4 Index (r = 0.33) is illustrated in **Figure 10(b)**, which underscores a more pronounced relationship between NDVI and ENSO events. Enhanced rainfall during El Niño events typically promotes vegetation growth, resulting in increased NDVI. Conversely, La Niña events, which are characterised by reduced rainfall and higher temperatures, often suppress vegetation. Notable examples include the 1997/1998 El Niño, which coincided with a strong Indian Ocean Dipole (IOD) and led to a significant rise in precipitation and NDVI, compared to the 2015 El Niño, which had a weaker impact due to the absence of a strong IOD (MacLeod & Caminade, 2019; Slingo & Annamalai, 2000).

Extremely weak correlation between NDVI and the Atlantic Multidecadal Oscillation (AMO) (r = 0.03) is Illutsrated in **Figure 10(c)**, indicating that the AMO exerts a negligible influence on East African vegetation dynamics. This weak teleconnection is likely attributable to the geographic distance and limited interaction between the AMO and East African climatic conditions, further underscoring the dominance of more proximate climatic drivers such as ENSO and IOD. These findings collectively highlight the varying degrees of influence that climatic indices exert on NDVI, underscoring the necessity to account for both individual and combined effects in understanding vegetation dynamics.

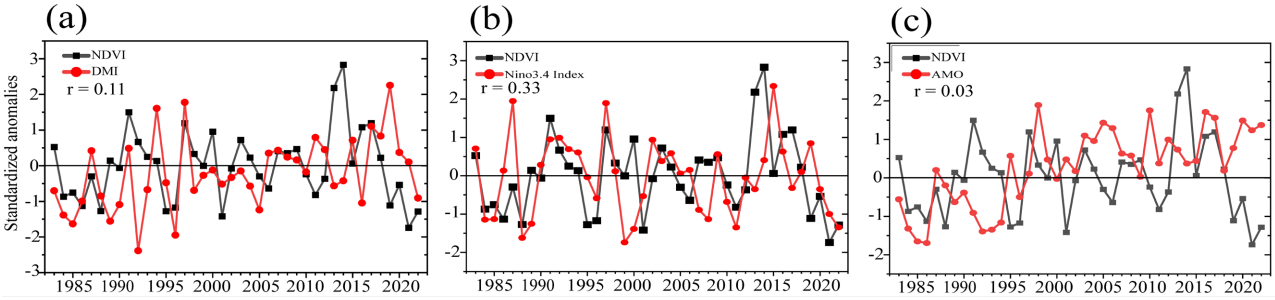

Figure 10. Illustrates the annual correlation between Normalized NDVI and (a) DMI (b) Nino 3.4 Index and (c) AMO over the period 1983 to 2022.

3.4. Discussion

This study examines the interannual variability of NDVI in response to climate factors. The annual mean time series of NDVI demonstrates interannual variability, with the highest value recorded in 1998 at 0.53 and the lowest in 2022 at 0.47 (**Figure 2(a)**). The spatial climatological values of NDVI across the majority of East Africa are predominantly within the range of 0.2 to 0.6, as illustrated in **Figure 2(b)**. These values indicate areas of moderate vegetation. The highest values were observed in southern and western Tanzania, Uganda, Rwanda and Burundi, while the lowest NDVI values were found in Kenya, northern and central Tanzania.

The occurrence of wet and drought years was determined through the normalization of NDVI. A total of eight (8) years were classified as wet years, based

on the criterion of a standardized anomaly greater than +0.5. The years in question are 1990, 1997, 1998, 2002, 2007, 2008, 2018, and 2020. Conversely, eleven (11) years were identified as drought years, with values less than -0.5: 1983, 1984, 1988, 1991, 2000, 2005, 2009, 2015, 2017, 2021, and 2022 (**Figure 3** and **Table 1**).

A composite analysis was conducted to investigate the spatial differences between wet years and drought years in terms of NDVI and climatic factors. A positive difference indicates an increase in NDVI during wet years, whereas a negative difference indicates a decrease compared to drought years. The results indicated that the NDVI values were positive in Kenya, Central and Northeastern Tanzania, indicating that NDVI values were higher during wet years than during drought years. This result is consistent with the hypothesis that increased vegetation cover during periods of increased rainfall over the region is parallel to those explained by Parracciani et al. (2023). This is associated with low incoming solar radiation in these areas (as indicated by low SLHF) (**Figure 5(f)**), high SSHF leads to increased outgoing solar radiation (**Figure 5(c)**), which contributes to lower air temperatures (**Figure 6(f)**), alongside moderate to high precipitation (**Figure 6(c)**) and moderate to high soil moisture (**Figure 7(c)**). Furthermore, low soil temperatures (**Figure 7(f)**) also play a role in this dynamic. Collectively, these factors have contributed to the rise in NDVI values across these areas (**Figure 4(c)**).

In contrast, the decline in NDVI values across Uganda, Rwanda, Burundi, the western and southern regions of Tanzania indicates that during wet years, there were fewer NDVI values compared to drought years. This decline is associated with high SLHF over these areas (**Figure 5(f)**), which leads to increased evaporation and evapotranspiration, and low SSHF (**Figure 5(c)**), indicating reduced outgoing solar radiation. This combination of factors results in warmer surface temperatures (**Figure 6(f)**) and elevated soil temperatures (**Figure 7(f)**), which ultimately cause lower soil moisture levels (**Figure 7(c)**). Furthermore, the precipitation levels in these regions are low (**Figure 6(c)**), which serves to intensify the conditions that lead to a reduction in NDVI values (**Figure 4(c)**).

The results of the correlation analysis indicated the existence of statistically significant relationships between the NDVI and a number of climatic factors. In particular, the NDVI demonstrated negative correlations with SLHF, which is consistent with the findings of Bateni et al. (2014). The result aligns with the previous findings of Sun and Kafatos (2007) and Runke et al. (2022) regarding negative correlation with air temperature. Additionally, the result is analogous to that of Zaitchik et al. (2007) regarding negative correlation with soil temperature. Conversely, positive correlations were identified with SSHF, precipitation, the result aligning with the findings of Davenport and Nicholson (1993), and soil moisture, the result corroborating the findings of McNally et al. (2013).

Furthermore, teleconnections with large-scale climate indices indicated modest correlations that contribute to the variability of NDVI. The Niño 3.4 index

demonstrated a correlation coefficient of $r = 0.33$, while the Indian Ocean Dipole Mode Index (DMI) and the Atlantic Multidecadal Oscillation (AMO) exhibited coefficients of $r = 0.11$ and $r = 0.03$, respectively. These findings underscore the complex interactions between NDVI and climatic conditions.

4. Conclusion

The research examined the interannual variability of the NDVI in relation to its interaction with climatic factors across East Africa from 1983 to 2022, utilizing monthly data sets. The NDVI data were obtained from the GIMMS database. The objective was to gain insights into the annual variation in NDVI and its relationship with climatic factors. The following conclusions were drawn:

1) The analysis demonstrates the difference between wet years and drought years, indicating an increase in NDVI values across Kenya, central and northeastern Tanzania. This suggests that during wet years, greater NDVI values were acquired compared to drought years, which reflects enhanced vegetative growth. This increase is primarily attributed to reductions in SLHF, increases in SSHF, cooler air temperatures, moderate precipitation, enhanced soil moisture, and lower soil temperatures. Furthermore, warmer SST anomalies in the equatorial Pacific contributed to heightened atmospheric moisture levels, transported to East Africa by strong westerly winds, thereby facilitating precipitation and promoting vegetation growth. In contrast, a decline in vegetation was observed in Uganda, Rwanda, Burundi, western and southern regions of Tanzania. This suggests that during wet years, less NDVI values were obtained compared to drought years, which reflects stress in vegetation. This is likely due to adverse climatic conditions characterized by high SLHF, less SSHF, and diminished precipitation, resulting in lower soil moisture and elevated temperatures.

2) The study also demonstrates the influence of large-scale climatic phenomena, such as the Atlantic Multidecadal Oscillation (AMO), the Dipole Mode Index (DMI), and the El Niño-Southern Oscillation (ENSO), on NDVI variability. While the AMO exhibited a relatively weak influence, both the DMI and ENSO demonstrated significant impacts, especially when their effects coincided. These findings underscore the importance of large-scale teleconnections in shaping annual vegetation dynamics across East Africa.

However, this study's limitations are acknowledged, including its exclusive focus on annual responses to climatic factors while overlooking monthly and seasonal variations. Future research should incorporate these dimensions to provide a more detailed understanding of NDVI variations in the region. In order to address the challenges posed by vegetation changes, this study proposes the implementation of continuous monitoring programmes and the development of predictive models for NDVI and associated climatic factors. Such initiatives would enhance our capability to anticipate vegetation shifts and facilitate the implementation of adaptive strategies to mitigate the negative impacts of climate change.

Acknowledgements

We, the authors, express our sincere gratitude to the National Oceanic and Atmospheric Administration (NOAA), the European Centre for Medium-Range Weather Forecasts (ECMWF) (ERA5), and the Climate Research Unit (CRU) for providing the datasets used in this study. We also extend our appreciation to the Tanzania Meteorological Authority and the Ministry of Commerce of China (MOFCOM) for facilitating this research opportunity.

Conflict of Interest

The authors confirm that there are no conflicts of interest associated with the publication of this paper.

References

Aguilar, C., Zinnert, J. C., Polo, M. J., & Young, D. R. (2012). NDVI as an Indicator for Changes in Water Availability to Woody Vegetation. *Ecological Indicators, 23,* 290-300. https://doi.org/10.1016/j.ecolind.2012.04.008

Areffian, A., Eslamian, S., Sadr, M. K., & Khoshfetrat, A. (2021). Monitoring the Effects of Drought on Vegetation Cover and Ground Water Using MODIS Satellite Images and Ann. *KSCE Journal of Civil Engineering, 25,* 1095-1105. https://doi.org/10.1007/s12205-021-2062-x

ASMET (2019). *2009 Drought in East Africa. Africa Satelite Meteorology Education and Training.*

Ayugi, B., Dike, V., Ngoma, H., Babaousmail, H., Mumo, R., & Ongoma, V. (2021). Future Changes in Precipitation Extremes over East Africa Based on CMIP6 Models. *Water, 13,* Article2358. https://doi.org/10.3390/w13172358

Bateni, S. M., Entekhabi, D., Margulis, S., Castelli, F., & Kergoat, L. (2014). Coupled Estimation of Surface Heat Fluxes and Vegetation Dynamics from Remotely Sensed Land Surface Temperature and Fraction of Photosynthetically Active Radiation. *Water Resources Research, 50,* 8420-8440. https://doi.org/10.1002/2013wr014573

Bonan, G. B. (2008). Forests and Climate Change: Forcings, Feedbacks, and the Climate Benefits of Forests. *Science, 320,* 1444-1449. https://doi.org/10.1126/science.1155121

Borhara, K., Pokharel, B., Bean, B., Deng, L., & Wang, S. S. (2020). On Tanzania's Precipitation Climatology, Variability, and Future Projection. *Climate, 8,* Article 34. https://doi.org/10.3390/cli8020034

Cane, M. A. (1983). Oceanographic Events during El Niño. *Science, 222,* 1189-1195. https://doi.org/10.1126/science.222.4629.1189

Chang'a, L. B., Kijazi, A. L., Luhunga, P. M., Ng'ongolo, H. K., & Mtongor, H. I. (2017). Spatial and Temporal Analysis of Rainfall and Temperature Extreme Indices in Tanzania. *Atmospheric and Climate Sciences, 7,* 525-539. https://doi.org/10.4236/acs.2017.74038

Clark, C. O., Webster, P. J., & Cole, J. E. (2003). Interdecadal Variability of the Relationship between the Indian Ocean Zonal Mode and East African Coastal Rainfall Anomalies. *Journal of Climate, 16,* 548-554. https://doi.org/10.1175/1520-0442(2003)016<0548:ivotrb>2.0.co;2

Davenport, M. L., & Nicholson, S. E. (1993). On the Relation between Rainfall and the Normalized Difference Vegetation Index for Diverse Vegetation Types in East Africa.

International Journal of Remote Sensing, 14, 2369-2389. https://doi.org/10.1080/01431169308954042

Diallo, I., Giorgi, F., & Stordal, F. (2018). Influence of Lake Malawi on Regional Climate from a Double-Nested Regional Climate Model Experiment. *Climate Dynamics, 50,* 3397-3411. https://doi.org/10.1007/s00382-017-3811-x

Ding, M., Zhang, Y., Liu, L., Zhang, W., Wang, Z., & Bai, W. (2007). The Relationship between NDVI and Precipitation on the Tibetan Plateau. *Journal of Geographical Sciences, 17,* 259-268. https://doi.org/10.1007/s11442-007-0259-7

Duveiller, G., Hooker, J., & Cescatti, A. (2018). The Mark of Vegetation Change on Earth's Surface Energy Balance. *Nature Communications, 9,* Article No. 679. https://doi.org/10.1038/s41467-017-02810-8

Fu, C., Hao, H., Li, T., Li, Y., & Yang, F. (2024). Lag Effects of Vegetation of Temperature Stress on and Its Ecological Risk Assessment. *Frontiers in Environmental Science, 12,* Article 1424578. https://doi.org/10.3389/fenvs.2024.1424578

Gessesse, A. A., & Melesse, A. M. (2019). Temporal Relationships between Time Series Chirps-Rainfall Estimation and eMODIS-NDVI Satellite Images in Amhara Region, Ethiopia. In A. M. Melesse, W. Abtew, & G. Senay (Eds.), *Extreme Hydrology and Climate Variability* (pp. 81-92). Elsevier. https://doi.org/10.1016/b978-0-12-815998-9.00008-7

Ghebrezgabher, M. G., Yang, T., Yang, X., & Eyassu Sereke, T. (2020). Assessment of NDVI Variations in Responses to Climate Change in the Horn of Africa. *The Egyptian Journal of Remote Sensing and Space Science, 23,* 249-261. https://doi.org/10.1016/j.ejrs.2020.08.003

Gilbert Ouma (2024). *Kenya's Had Unusually Hot Weather—An Expert Unpacks What Could Be Causing It.* PreventionWeb.

Gore, S. M., Jones, I. G., & Rytter, E. C. (1977). Misuse of Statistical Methods: Critical Assessment of Articles in BMJ from January to March 1976. *BMJ, 1,* 85-87. https://doi.org/10.1136/bmj.1.6053.85

Gray, M. A., McGowan, H. A., Lowry, A. L., & Guyot, A. (2018). Surface Energy Exchanges over Contrasting Vegetation Types on a Sub-Tropical Sand Island. *Agricultural and Forest Meteorology, 249,* 81-99. https://doi.org/10.1016/j.agrformet.2017.11.018

Habib, E., Krajewski, W. F., & Ciach, G. J. (2001). Estimation of Rainfall Interstation Correlation. *Journal of Hydrometeorology, 2,* 621-629. https://doi.org/10.1175/1525-7541(2001)002<0621:eoric>2.0.co;2

Han, W., Chen, D., Li, H., Chang, Z., Chen, J., Ye, L. et al. (2022). Spatiotemporal Variation of NDVI in Anhui Province from 2001 to 2019 and Its Response to Climatic Factors. *Forests, 13,* Article 1643. https://doi.org/10.3390/f13101643

Harris, I., Osborn, T. J., Jones, P., & Lister, D. (2020). Version 4 of the CRU TS Monthly High-Resolution Gridded Multivariate Climate Dataset. *Scientific Data, 7,* Article No. 109. https://doi.org/10.1038/s41597-020-0453-3

IOM (2023). *Horn of Africa Drought 2022: Human Mobility Snap-Shot.*

Kalisa, W., Igbawua, T., Henchiri, M., Ali, S., Zhang, S., Bai, Y. et al. (2019). Assessment of Climate Impact on Vegetation Dynamics over East Africa from 1982 to 2015. *Scientific Reports, 9,* Article No. 16865. https://doi.org/10.1038/s41598-019-53150-0

Kalisa, W., Igbawua, T., Ujoh, F., Aondoakaa, I. S., Namugize, J. N., & Zhang, J. (2021). Spatio-temporal Variability of Dry and Wet Conditions over East Africa from 1982 to 2015 Using Quantile Regression Model. *Natural Hazards, 106,* 2047-2076. https://doi.org/10.1007/s11069-021-04530-1

Kavishe, G. M., & Limbu, P. T. S. (2020). Variation of October to December Rainfall in Tanzania and Its Association with Sea Surface Temperature. *Arabian Journal of Geosciences, 13,* Article No. 534. https://doi.org/10.1007/s12517-020-05535-z

Kijazi, A., & Reason, C. (2009). Analysis of the 1998 to 2005 Drought over the Northeastern Highlands of Tanzania. *Climate Research, 38,* 209-223. https://doi.org/10.3354/cr00784

Kim, I., Stuecker, M. F., Timmermann, A., Zeller, E., Kug, J., Park, S. et al. (2021). Tropical Indo-Pacific SST Influences on Vegetation Variability in Eastern Africa. *Scientific Reports, 11,* Article No. 10462. https://doi.org/10.1038/s41598-021-89824-x

Kimani, M., Hoedjes, J., & Su, Z. (2017). An Assessment of Satellite-Derived Rainfall Products Relative to Ground Observations over East Africa. *Remote Sensing, 9,* Article 430. https://doi.org/10.3390/rs9050430

Koutsouris, A. J., Chen, D., & Lyon, S. W. (2016). Comparing Global Precipitation Data Sets in Eastern Africa: A Case Study of Kilombero Valley, Tanzania. *International Journal of Climatology, 36,* 2000-2014. https://doi.org/10.1002/joc.4476

Kraetzig, N. M. (2022). *Things to Know about NDVI (Normalized Difference Vegetation Index).* UP42 Official Website.

MacLeod, D., & Caminade, C. (2019). The Moderate Impact of the 2015 El Niño over East Africa and Its Representation in Seasonal Reforecasts. *Journal of Climate, 32,* 7989-8001. https://doi.org/10.1175/jcli-d-19-0201.1

Mao, X., Ren, H., & Liu, G. (2022). Primary Interannual Variability Patterns of the Growing-Season NDVI over the Tibetan Plateau and Main Climatic Factors. *Remote Sensing, 14,* Article 5183. https://doi.org/10.3390/rs14205183

McNally, A., Funk, C., Husak, G. J., Michaelsen, J., Cappelaere, B., Demarty, J., Pellarin, T., Young, T. P., Caylor, K. K., Riginos, C., & Veblen, K. E. (2013). Estimating Sahelian and East African Soil Moisture Using the Normalized Difference Vegetation Index. https://doi.org/10.5194/hessd-10-7963-2013

Nicholson, S. E., Davenport, M. L., & Malo, A. R. (1990). A Comparison of the Vegetation Response to Rainfall in the Sahel and East Africa, Using Normalized Difference Vegetation Index from NOAA AVHRR. *Climatic Change, 17,* 209-241. https://doi.org/10.1007/bf00138369

Ongoma, V., & Chen, H. (2017). Temporal and Spatial Variability of Temperature and Precipitation over East Africa from 1951 to 2010. *Meteorology and Atmospheric Physics, 129,* 131-144. https://doi.org/10.1007/s00703-016-0462-0

Palmer, P. I., Wainwright, C. M., Dong, B., Maidment, R. I., Wheeler, K. G., Gedney, N. et al. (2023). Drivers and Impacts of Eastern African Rainfall Variability. *Nature Reviews Earth & Environment, 4,* 254-270. https://doi.org/10.1038/s43017-023-00397-x

Pang, G., Chen, D., Wang, X., & Lai, H. (2022). Spatiotemporal Variations of Land Surface Albedo and Associated Influencing Factors on the Tibetan Plateau. *Science of the Total Environment, 804,* Article ID: 150100. https://doi.org/10.1016/j.scitotenv.2021.150100

Parracciani, C., Buitenwerf, R., & Svenning, J. (2023). Impacts of Climate Change on Vegetation in Kenya: Future Projections and Implications for Protected Areas. *Land, 12,* Article 2052. https://doi.org/10.3390/land12112052

Paruelo, J. M., & Lauenroth, W. K. (1998). Interannual Variability of NDVI and Its Relationship to Climate for North American Shrublands and Grasslands. *Journal of Biogeography, 25,* 721-733. https://doi.org/10.1046/j.1365-2699.1998.2540721.x

Philander, S. G. H. (1983). El Niño Southern Oscillation Phenomena. *Nature, 302,* 295-301. https://doi.org/10.1038/302295a0

Pregitzer, K. S., & King, J. S. (2005). Effects of Soil Temperature on Nutrient Uptake. In H.

BassiriRad (Ed.), *Nutrient Acquisition by Plants* (pp. 277-310). Springer-Verlag. https://doi.org/10.1007/3-540-27675-0_10

Rasmusson, E. M., & Wallace, J. M. (1983). Meteorological Aspects of the El Niño/Southern Oscillation. *Science, 222,* 1195-1202. https://doi.org/10.1126/science.222.4629.1195

Runke, W., Xiaoni, Y., Yaya, S., Chengyong, W., & Baokang, L. (2022). Study on Air Temperature Estimation and Its Influencing Factors in a Complex Mountainous Area. *PLOS ONE, 17,* e0272946. https://doi.org/10.1371/journal.pone.0272946

Sheriff, A. (2017). The Swahili in the African and Indian Ocean Worlds to c. 1500. In *Oxford Research Encyclopedia of African History*. Oxford University Press. https://doi.org/10.1093/acrefore/9780190277734.013.152

Slingo, J. M., & Annamalai, H. (2000). 1997: The El Niño of the Century and the Response of the Indian Summer Monsoon. *Monthly Weather Review, 128,* 1778-1797. https://doi.org/10.1175/1520-0493(2000)128<1778:tenoot>2.0.co;2

Sonia,, Sunita,, Ghosh, T., Amari, A., Yadav, V. K., Osman, H. et al. (2023). Appraisal of Long-Term Responsiveness of Normalized Difference Vegetation Index to Climatic Factors Using Multiscale Time-Frequency Decomposition in an Arid Environment. *Frontiers in Earth Science, 11,* Article 1265292. https://doi.org/10.3389/feart.2023.1265292

Su, Y., Zhang, C., Chen, X., Liu, L., Ciais, P., Peng, J. et al. (2021). Aerodynamic Resistance and Bowen Ratio Explain the Biophysical Effects of Forest Cover on Understory Air and Soil Temperatures at the Global Scale. *Agricultural and Forest Meteorology, 308,* Article ID: 108615. https://doi.org/10.1016/j.agrformet.2021.108615

Sun, D., & Kafatos, M. (2007). Note on the NDVI-LST Relationship and the Use of Temperature-Related Drought Indices over North America. *Geophysical Research Letters, 34,* L24406. https://doi.org/10.1029/2007gl031485

Tucker, C. J., Pinzon, J. E., Brown, M. E., Slayback, D. A., Pak, E. W., Mahoney, R. et al. (2005). An Extended AVHRR 8-km NDVI Dataset Compatible with MODIS and SPOT Vegetation NDVI Data. *International Journal of Remote Sensing, 26,* 4485-4498. https://doi.org/10.1080/01431160500168686

van Heerwaarden, C. C., & Teuling, A. J. (2014). Disentangling the Response of Forest and Grassland Energy Exchange to Heatwaves under Idealized Land-Atmosphere Coupling. *Biogeosciences, 11,* 6159-6171. https://doi.org/10.5194/bg-11-6159-2014

Walther, G., Post, E., Convey, P., Menzel, A., Parmesan, C., Beebee, T. J. C. et al. (2002). Ecological Responses to Recent Climate Change. *Nature, 416,* 389-395. https://doi.org/10.1038/416389a

Ward, N., Walker, D. P., Keane, R. J., Marsham, J. H., Scaife, A. A., Birch, C. E. et al. (2023). Predictability of the East Africa Long Rains through Congo Zonal Winds. *Atmospheric Science Letters, 24,* e1185. https://doi.org/10.1002/asl.1185

Yang, X., Yang, T., Ji, Q., He, Y., & Ghebrezgabher, M. G. (2014). Regional-scale Grassland Classification Using Moderate-Resolution Imaging Spectrometer Datasets Based on Multistep Unsupervised Classification and Indices Suitability Analysis. *Journal of Applied Remote Sensing, 8,* Article ID: 083548. https://doi.org/10.1117/1.jrs.8.083548

Zaitchik, B. F., Evans, J. P., Geerken, R. A., & Smith, R. B. (2007). Climate and Vegetation in the Middle East: Interannual Variability and Drought Feedbacks. *Journal of Climate, 20,* 3924-3941. https://doi.org/10.1175/jcli4223.1

Zhang, J., Yang, T., Deng, M., Huang, H., Han, Y., & Xu, H. (2023). Spatiotemporal Variations and Its Driving Factors of NDVI in Northwest China during 2000-2021. *Environmental Science and Pollution Research, 30,* 118782-118800.

https://doi.org/10.1007/s11356-023-30250-z

Zhang, M., Wang, J., & Li, S. (2019). Tempo-Spatial Changes and Main Anthropogenic Influence Factors of Vegetation Fractional Coverage in a Large-Scale Opencast Coal Mine Area from 1992 to 2015. *Journal of Cleaner Production, 232,* 940-952. https://doi.org/10.1016/j.jclepro.2019.05.334